Journal of Zhejiang University SCIENCE
ISSN 1009-3095
http://www.zju.edu.cn/jzus
E-mail: jzus@zju.edu.cn

$ZnS_{0.8}Se_{0.2}$ film for high resolution liquid crystal light valve*

SHEN Da-ke (沈大可)[†1,2], HAN Gao-rong (韩高荣)[†1], DU Pi-yi (杜丕一)[1],
QUE Duan-lin (阙端麟)[1], SOU I. K.[2]

([1]*State Key Laboratory of Silicon Material Science, Zhejiang University, Hangzhou 310027, China*)
([2]*Department of Physics, Hong Kong University of Science and Technology, Hong Kong, China*)
[†]E-mail: dake.shen@gepex.ge.com; hgr@zju.edu.cn
Received Aug. 21, 2002; revision accepted Jan. 6, 2003

Abstract: The structural characteristics and optical and electrical properties of molecular-beam-epitaxy (MBE) grown $ZnS_{0.8}Se_{0.2}$ thin films on indium-tin-oxide (ITO) glass substrates were investigated in this work. The *X*-ray diffraction (XRD) results indicated that high quality polycrystalline $ZnS_{0.8}Se_{0.2}$ thin film grown at the optimized temperature had a preferred orientation along the (111) planes. The transmission electron microscopy (TEM) cross-sectional micrograph of the sample showed a well defined columnar structure with lateral crystal dimension in the order of a few hundred angstroms. Ultraviolet (UV) photoresponsivity as high as 0.01 A/W had been demonstrated and for wavelengths longer than 450 nm, the response was down from the peak response by more than 3 orders of magnitude. The thin $ZnS_{0.8}Se_{0.2}$ photosensor layer, with a wide energy gap and anisotropic electrical property, makes a transmission UV liquid crystal light valve (LCLV) with high resolution feasible.

Key words: UV LCLV, Transmission mode, Polycrystalline $ZnS_{0.8}Se_{0.2}$ thin film, MBE
Document code: A **CLC number:** TN204

INTRODUCTION

Liquid crystal light valves (LCLV) are devices whose function is to convert an input image possessing specific wavelength, intensity and coherence to an output image in which some or all of these parameters are varied (Efron *et al*., 1985). Therefore, they can be used as image amplifiers for large screen projection display, image wavelength converters and incoherent-to-coherent image converters for optical data processing and correlation. The application potentialities are defined by the LCLV device's excellent operating characteristics, among which the input sensitivity, spatial resolution and response speed are important. Work was started on reflective light valve projectors by Hughes Electronics in the early 1970s, and more-or-less simultaneously, by AT&T Bell Labs. Different types of LCLVs using CdS/CdTe heterojunction (Natu and Casasent, 1979), GaAs (Armitage *et al*., 1989), Si (Efron *et al*., 1985), $Bi_{12}SiO_{20}$ (BSO) (Aubourg *et al*., 1982) and a-Si:H (Qiao *et al*., 1991) as the photosensitive layer had been studied and fabricated in the past 30 years. However, nearly all of them were used in the visible to infrared spectrum region. ZnS-based II-VI wide-band-gap semiconductors offer opportunity for developing opto-electronic devices that can combine high sensitivity in the ultraviolet (UV) region with negligible sensitivity in the visible region. The authors recently demonstrated that the molecular beam epitaxy (MBE) grown polycrystalline ZnS_xSe_{1-x} thin films on in-

* Project supported by the National Natural Science Foundation of China (No. 59910161981) and RGC grant from the Hong Kong Government Grant (No. NSFC/HKUST 35), China

dium-tin-oxide (ITO) coated glass had the potential to fulfill the demanding requirements of a novel visible blind UV LCLV in reflection mode because of its good photo-to-dark impedance ratio, large area coverage, tunable wavelength response, thin film type and low temperature deposition (Shen *et al*., 2001). To expand the availability of LCLV in optical information processing and optical computing, researchers have also desired an LCLV operating in a transmission mode. In this work, we focus our attention on the structural characteristics and optical and electrical properties of the columnar $ZnS_{0.8}Se_{0.2}$ thin film with (111) planes preferred orientation used for high-resolution UV LCLV in transmission mode.

EXPERIMENT

$ZnS_{0.8}Se_{0.2}$ thin films used in this study were fabricated using a VG V80H MBE system. The pre-growth treatment of the substrate is essential for obtaining high quality $ZnS_{0.8}Se_{0.2}$ thin film. Commercial ITO coated quartz glass substrates were first cleaned using Decon 90 detergent and then rinsed in de-ionized water (18.2 MΩcm) in an ultrasonic bath for 30 minutes at 40 ºC. After being baked dry at 100 ºC for 1 hour, they were loaded into the MBE system. Prior to the deposition, the substrates were pre-heated at 380 ºC for 20 minutes. The growth of $ZnS_{0.8}Se_{0.2}$ thin films was carried out using ZnS and ZnSe compound sources. The substrate temperature was kept at 280 ºC. More detailed information about the growth conditions can be found elsewhere (Shen *et al*., 2002). The as-grown thin film was cut into several pieces for various structural characterizations. Crystallinity of the films was examined using a Philips PW1830 powder *X*-ray diffraction (XRD) system which uses the Cu Kα radiation (λ=1.540562 Å). Standard $\theta/2\theta$ scans were performed with 2θ ranging from 15º to 65º. To investigate the microstructure of the film, high quality cross sectional specimens with minimum damage for transmission electron microscopy (TEM) study were prepared first by mechanical polishing and then argon ion milling with successively decreasing ion-accelerating voltage. The cross sectional images were then taken in a Philips CM20 TEM at 200 kV. Photocurrent responsivity measurements were carried out on a set of Au arrays with the thickness of 100 Å as the top transparent electrode. The light source was provided by a 150 W xenon arc lamp. The light beam was first dispersed using a monochromator and then focused onto the mesa area. At each wavelength, the power of the light incident on the mesa was carefully measured using a Newport 835 optical power meter that uses a UV-enhanced Si photodiode (818UV) as the detector. The spectral response of this power meter had been calibrated by the manufacturer. The short-circuit photocurrent was measured using a digital current meter (Keithley model 237) with high sensitivity and precision. For the dark conductivity measurements, arrays of either Au or In cells each with thickness of 2000 Å were fabricated as the top electrode using the radio-frequency (RF) sputtering technique and standard photolithography.

DEVICE CONFIGURATION AND MECHANISM

The UV LCLV in transmission mode has a simple structure consisting of a $ZnS_{0.8}Se_{0.2}$ photosensitive layer and a liquid crystal layer sandwiched by two ITO coated quartz glass substrates as the transparent electrode. The input UV optical image activates the $ZnS_{0.8}Se_{0.2}$ photosensor, which produces a corresponding charge image that provides the electric field for the liquid crystal material. Modulation of the readout light is achieved by successive passes through the liquid crystal element in a transmission scheme. A cross section of the transmission UV LCLV is illustrated in Fig.1. It can be proved (Du *et al*., 1992) that at d.c. operation, the voltage drop across the liquid-crystal layer, V_{LC}, under a total applied bias V is given by

$$V_{LC} \approx \frac{V}{\frac{R_{PS}^{DY}}{R_{LC}} + 1} \tag{1}$$

where R_{LC}, resistance of the liquid crystal layer; R_{PS}^{D}, dark resistance of the photosensor layer; Y, direction perpendicular to the photosensor and liquid crystal

layers. Eq.(1) indicates that in order to efficiently modulate the voltage across the LC layer, R_{PS}^{DY} should be of the same order as R_{LC}. Considering the same area and nearly same thickness of the photosensor and liquid crystal layer, this also means the conductivity of these two layers should be in the same order.

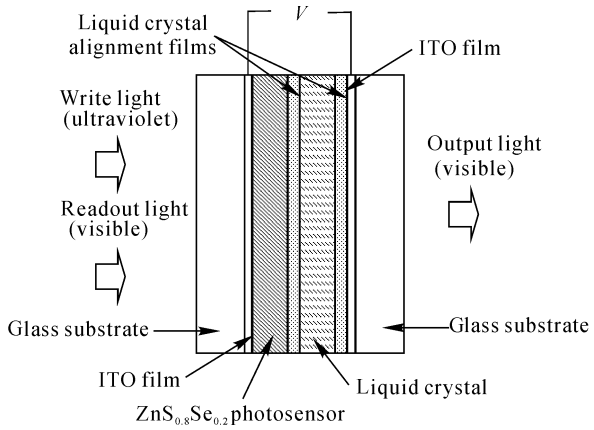

Fig.1 Cross sectional view of the $ZnS_{0.8}Se_{0.2}$ UV LCLV in a transmission mode

The signal charge (electron) spread in the photosensor is a main factor affecting the resolution. The lateral spread of the signal charge due to diffusion is given by

$$L = \sqrt{Dt} \tag{2}$$

Where L, the radius of diffusion; D, diffusion coefficient; t, spread time.

Using the Einstein relationship:

$$D = kT\mu_X/\mathrm{e}, \tag{3}$$

where μ_X, charge carrier mobility parallel to the photosensor layer;

$$t = d_{PS}^2 /\mu_Y V_{PS}, \tag{4}$$

where d_{PS}, the thickness of photosensor; V_{PS}, voltage drop in photosensor; μ_Y, charge carrier mobility perpendicular to the photosensor layer.

We have

$$2L = 2d_{PS}\sqrt{kT\mu_X/\mathrm{e}V_{PS}\mu_Y} \tag{5}$$

as the effective charge spreading in the $ZnS_{0.8}Se_{0.2}$ photosensor layer.

Eq.(5) indicates that high resolution is associated with thin photosensor layer and the low ratio of μ_X/μ_Y. In the first approximation, based on the all loss mechanisms of the device, the ratio of the device resolution with an anisotropic and isotropic photosensor respectively can be described as (Vladimirov *et al*., 1996):

$$\frac{S_A}{S_I} = \sqrt{\frac{\sigma_{LC}d_{LC} + \sigma_{PS}^{DY}d_{PS}}{\sigma_{LC}d_{LC} + \sigma_{PS}^{DX}d_{PS}}} \tag{6}$$

where d_{LC}, thickness of liquid crystal layer; σ_{LC}, conductivity of liquid crystal layer; X, direction parallel to the photosensor and liquid crystal layers; S_A and S_I, the device resolution with an anisotropic photosensor ($\sigma_{PS}^{DY} > \sigma_{PS}^{DX}$) and isotropic photosensor ($\sigma_{PS}^{DY} = \sigma_{PS}^{DX}$), respectively.

Eq.(6) again indicates larger σ_{PS}^{DY} than σ_{PS}^{DX} in the photosensor will improve the resolution of the device as compared to an isotropic structural photosensor with $\sigma_{PS}^{DY} = \sigma_{PS}^{DX}$.

RESULTS

In our previous studies, we found the structural characteristics of the polycrystalline ZnS_xSe_{1-x} thin film strongly depend on the growth temperature (Shen *et al*., 2002). High quality $ZnS_{0.8}Se_{0.2}$ thin film was obtained under the optimized temperature of 280 ºC. The photocurrent responsivity at zero bias measured for the sample achieved a peak responsivity of about 0.01 A/W at 360 nm. Fig.2 shows the photocurrent response as a function of the incident photon wavelength for $ZnS_{0.8}Se_{0.2}$ thin film. The responsivity has a rather sharp transition; in fact, for wavelengths longer than 450 nm, the response is down from the peak response by more than 3 orders of magnitude, showing very good visible rejection. The significant drop in the short wavelength end of the photoresponse as shown in Fig.2 cannot be fully explained by the reduction of the incoming photons per unit power as the wavelength decreases. We be-

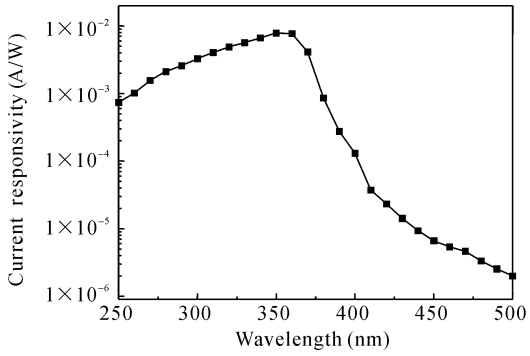

Fig.2 Photocurrent responsivity as a function of photon wavelength of $ZnS_{0.8}Se_{0.2}$ sample

lieved that this observation may be attributed to the shallow penetration depth of short-wavelength UV radiation leading to a more significant loss of photo-carriers due to recombination at defects and grain boundaries of the film. Fig.3 shows the spectral transmittance of the $ZnS_{0.8}Se_{0.2}$ / ITO layer measured with a UV/VIS spectrophotometer (Lambda 20). The $ZnS_{0.8}Se_{0.2}$ / ITO layer shows a high transmittance (>60%) for light wavelength longer than 400 nm. These results showed that $ZnS_{0.8}Se_{0.2}$ thin film can be used in a transmission mode UV LCLV with read-out wavelength longer than 450 nm.

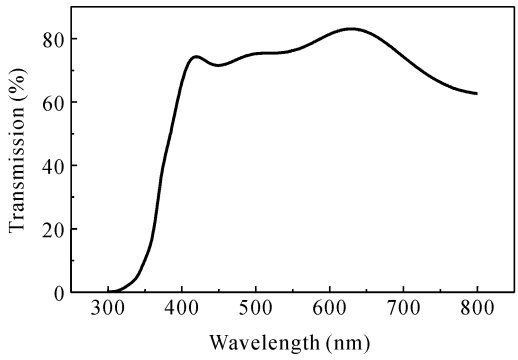

Fig.3 Spectral transmittance of the $ZnS_{0.8}Se_{0.2}$/ITO layer

Fig.4a and 4b show the *X*-ray diffraction patterns obtained for the ITO substrate and $ZnS_{0.8}Se_{0.2}$ sample, respectively. From inspection of Fig.4, one can see that the diffraction patterns of the substrate shows the typical ITO fingerprints with the diffraction line from (400) plane being the dominant component. And the as-grown $ZnS_{0.8}Se_{0.2}$ thin film shows a single diffraction peak located near the

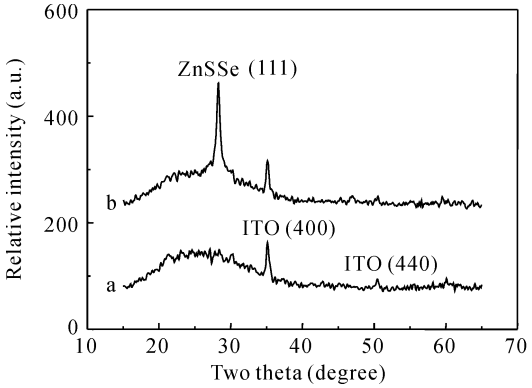

Fig.4 *X*-ray diffraction patterns of ITO substrate and $ZnS_{0.8}Se_{0.2}$ / ITO thin film
(a) ITO substrate (b) $ZnS_{0.8}Se_{0.2}$/ITO thin film

standard (111) peak of cubic ZnS at 2θ=28.5º. It is well known that pure ZnS and ZnSe exist in two crystalline phases, i.e., a cubic form with sphalerite structure and a hexagonal form with wurtzite structure. As to ZnS, the cubic form (c-ZnS) is the low temperature phase and the hexagonal form (h-ZnS) is the polymorph stable at high temperatures greater than 1020 ºC (Tagliente *et al*., 1999). Because there are usually just a few peaks in the diffractograms, and many d-values between the two phases are overlapped or only have very small difference, it is difficult to distinguish these two phases from thin film samples (Ihanus *et al*., 1997). However, absence of diffraction from any hexagonal planes indicated that the $ZnS_{0.8}Se_{0.2}$ thin film was polycrystalline with most probably zinc sulfide cubic structure and showed (111) preferred orientation. Fig.5 shows its cross-sectional TEM micrograph from which one can clearly see a well defined columnar structure grew from the substrate with lateral crystal dimension in the order of 500−650 angstroms.

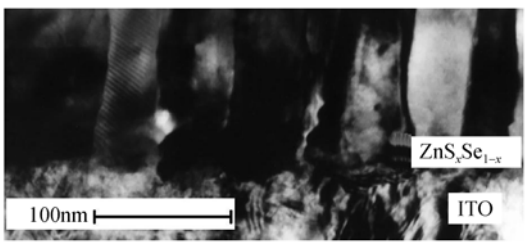

Fig.5 TEM cross sectional image of $ZnS_{0.8}Se_{0.2}$ / ITO thin film

Fig.6 shows the typical dark I-V plots measured perpendicular to the film. The ITO film was used as the bottom electrode. The I-V characteristics of the sample show a quasi-linear relationship for the bias range of −5 V to 5 V. At least five cells were taken from the sample for these measurements. The dark conductivity was extracted from a simple linear fitting of these I-V characteristics. These data indicated that the columnar $ZnS_{0.8}Se_{0.2}$ thin film had a larger longitudinal conductivity of 1.7×10^{-12} $(\Omega cm)^{-1}$ than the transverse conductivity of 3.6×10^{-13} $(\Omega cm)^{-1}$ measured by a high resistance meter (Model ZC 36). For polycrystalline thin films, it is believed that the carrier transport mechanism is dominated by carrier scattering through the inherent inter-crystalline boundaries, the so-called grain boundaries, rather than other intra-crystalline characteristics. The difference of the conductivity may be due to the anisotropic structure of the columnar $ZnS_{0.8}Se_{0.2}$ thin film with (111) preferred orientation. Since the conductivity of the LC layer used in LCLV devices was in the order of 10^{-12} $(\Omega cm)^{-1}$, one can see that the longitudinal conductivity of the $ZnS_{0.8}Se_{0.2}$ film is a very good match with the conductivity requirement as described in Eq.(1). Considering the low conductivity of the $ZnS_{0.8}Se_{0.2}$ thin film of 1.7×10^{-12} $(\Omega cm)^{-1}$ grown by MBE; the thin photosensor layer can be made to fit the resistance requirement of the device. This favors obtaining high resolution UV LCLV. What is more, the anisotropic conductivity of the photosensor improves the device resolution further as described before. An improvement of about 28% in the resolution of UV LCLV made by columnar $ZnS_{0.8}Se_{0.2}$ thin film has been obtained as compared to the normal one with isotropic structural photosensor. More detailed results of device characteristics will be reported elsewhere.

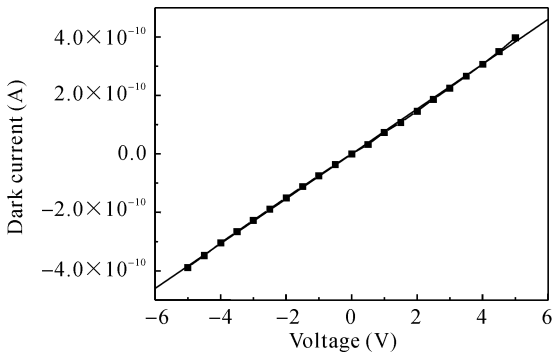

Fig.6 The typical longitudinal I-V plots obtained for $ZnS_{0.8}Se_{0.2}$ photosensor

CONCLUSION

In summary, investigation of various structural characterizations and optical and electrical properties of molecular-beam-epitaxy grown $ZnS_{0.8}Se_{0.2}$ thin film grown on indium-tin-oxide substrates was carried out. The sample grown at the optimized temperature of 280 ºC had a preferred orientation along (111) planes; and that its TEM cross-sectional micrograph had a well defined columnar structure. Room temperature photo-responsivity measurement performed on these thin films showed that the current responsivity in the UV spectral region was as high as 0.01 A/W; and that for wavelengths longer than 450 nm, the response was down from the peak response by more than 3 orders of magnitude. Anisotropic electrical property with longitudinal conductivity larger than the transverse conductivity had been obtained in the film. The thin $ZnS_{0.8}Se_{0.2}$ photosensor layer, with a wide energy gap and anisotropic electrical property, makes a transmission UV LCLV with high resolution feasible.

Reference

Armitage, D., Thackara, J.I., Eades, W.D., 1989. Photoaddressed liquid crystal spatial light modulators. *Appl. Opts*., **28**(22):4763-4771.

Aubourg, P., Huignard, J.P., Hareng, M., Mullen, R.A., 1982. Liquid crystal light valve using bulk monocrystalline $Bi_{12}SiO_{20}$ as the photoconductive material. *Appl. Opts*., **21**(20):3706-3712.

Du, P.Y., Han, G.R., Qiao, J.M., Han, W.Q., Zhao, D.M., Ding, Z.S., 1992. Investigation of optimal photosensor in a-Si:H liquid crystal light valves. *Mat. Res. Soc. Symp. Proc*., **258**:1175-1180.

Efron, U., Grinberg, J., Braatz, P.O., Little, M.J., Reif, P.G., Schwartz, R.N., 1985. The silicon liquid-crystal light valve. *J. Appl. Phys*., **57**(4):1356-1368.

Ihanus, J., Ritala, M., Leskelä, M., Rauhala, E., 1997. ALE growth of $ZnS_{1-x}Se_x$ thin films by substituting surface sulfur with elemental selenium. *Applied Surface Science*, **112**:154-158.

Natu, S., Casasent, D., 1979. Sensitometry control of a hybrid field-effect liquid crystal light valve. *Optics*

Communications, **31**(2):135-138.

Qiao, J.M., Han, G.R., Du, P.Y., Han, W.Q., Huang, W.Q., Ding, Z.S., 1991. Characterization of a-Si:H and a-SiGe:H films in liquid crystal light valve. *Mat. Res. Soc. Symp. Proc.*, **219**:179-184.

Shen, D.K., Au, S.Y., Han, G.R., Que, D.L., Sou, I.K., 2001. MBE-grown ZnSSe thin films on ITO substrates for liquid-crystal light valve applications. *Materials Science in Semiconductor Processing*, **4**(6):611-616.

Shen, D.K., Han, G.R., Que, D.L., Wong, G.K.L., Sou, I.K., 2002. Crystalline structure of MBE-grown ZnS_xSe_{1-x}/ITO thin films using compound sources. *Nanotechnology*, accepted.

Tagliente, M.A., Penza, M., Gusso, M., Quirini, A., 1999. Characterisation of ZnS:Mn thin films by Rietveld refinement of Bragg-Brentano *X*-ray diffraction patterns. *Thin Solid Films*, **353**:129-136.

Vladimirov, F.L., Morichev, I.E., Pletnieva, N.I., 1996. Influence of photoconductor parameters on characteristics of the spatial light modulators based on photoconductor-liquid crystal structures. *SPIE*, **2969**:278-282.